Toxicology and Applied Pharmacology 266 (2013) 56–66

Contents lists available at SciVerse ScienceDirect

Toxicology and Applied Pharmacology

journal homepage: www.elsevier.com/locate/ytaap

Comparative study of genotoxicity and tissue distribution of nano and micron sized iron oxide in rats after acute oral treatment

Shailendra Pratap Singh, M.F. Rahman, U.S.N. Murty, M. Mahboob, Paramjit Grover *

Toxicology Unit, Biology Division, Indian Institute of Chemical Technology, Hyderabad - 500 007, Andhra Pradesh, India

ARTICLE INFO

Article history:
Received 5 September 2012
Revised 25 October 2012
Accepted 29 October 2012
Available online 6 November 2012

Keywords:
Fe_2O_3-30 nm
Fe_2O_3-bulk
Genotoxicity
Comet assay
Micronucleus test
Chromosomal aberration assay
Biodistribution
Wistar rats

ABSTRACT

Though nanomaterials (NMs) are being utilized worldwide, increasing use of NMs have raised concerns over their safety to human health and environment. Iron oxide (Fe_2O_3) NMs have important applications. The aim of this study was to assess the genotoxicity of Fe_2O_3-30 nm and Fe_2O_3-bulk in female Wistar rats. Fe_2O_3-30 nm was characterized by using transmission electron microscopy, dynamic light scattering, laser Doppler velocimetry and surface area analysis. The rats were treated orally with the single doses of 500, 1000, 2000 mg/kg bw of Fe_2O_3-30 nm and Fe_2O_3 –bulk. The genotoxicity was evaluated at 6, 24, 48 and 72 h by the comet assay in leucocytes, 48 and 72 h by micronucleus test (MNT) in peripheral blood cells, 18 and 24 h by chromosomal aberration (CA) assay and 24 and 48 h by MNT in bone marrow cells. The biodistribution of iron (Fe) was carried out at 6, 24, 48 and 72 h after treatment in liver, spleen, kidney, heart, brain, bone marrow, urine and feces by using atomic absorption spectrophotometry.

The % tail DNA, frequencies of micronuclei and CAs were statistically insignificant ($p > 0.05$) at all doses. These results suggest that Fe_2O_3-30 nm and Fe_2O_3-bulk was not genotoxic at the doses tested.

Bioavailability of Fe was size and dose dependent in all the tissues from the groups exposed to Fe_2O_3-30 nm. Fe_2O_3 NMs were able to enter in the organs and the rats are biocompatible with much higher concentration of Fe. However, the accumulated Fe did not cause significant genotoxicity. This study provides additional knowledge about the toxicology of Fe_2O_3 NMs.

1. Introduction

Nanotechnology is the design, characterisation, production and application of structures, devices and systems by controlling shape and size at nanometer scale. Nanomaterials (NMs) are defined as nanoscale substances having one critical dimension less than 100 nanometres. Mankind stands to derive great benefit from nanotechnology. However, it is important to consider the potential health impact of NMs. Although no human ailments have been ascribed to NMs so far, early experimental studies indicate that NMs could initiate adverse biological responses that could lead to toxicological outcomes (Xie et al., 2009). There is valid cause for worry about NMs as many are new and untested. It has been demonstrated that treating mice with carbon nanotube by injection route its abdominal cavity produced effects similar to that caused by asbestos fibers (Poland et al., 2008). In contrast to the bulk materials some NMs may reach the nucleus and mitochondria (Geiser et al., 2005; Muhlfeld et al., 2007). Many intracellular NMs are membrane bound, and it can be assumed that this appear in cells by traditional endocytic mechanism. However, it is possible for NMs to enter in to the cells by non-tradition mechanism eg. non-endocytic pathways (Lewinski et al., 2008; Verma et al., 2008). Micro sized particles are mainly found in the cytoplasm mostly membrane bound within phagosomes of macrophages (Brain, 1985). On the contrary, the entry of NMs in to cells by non endocytic mechanism has been shown where they are found in the cytoplasm not enclosed by membranes (Geiser et al., 2005).

Metal oxides below 100 nm in size in at least one dimension are presently the most important tools applied for diagnosis of diseases, drug delivery systems, antimicrobials and as thermotherapy agents. They are also used in sunscreens, cosmetics, plastic wares, electrical appliances, food products, textiles, defence and agriculture. The innumerable applications of NMs due to their special physiochemical character give rise to a huge probability for human exposure. Hence they can be ingested directly via water, food, cosmetics, drugs, drug delivery devices, etc. (Oberdörster et al., 2005).

The nano sized iron oxide (Fe_2O_3) are of special importance because of their wide application such as magnetic resonance imaging (MRI) for contrast enhancement to identify metastatic from inflammatory

Abbreviations: TEM, Transmission electron microscopy; DLS, dynamic light scattering; LDV, laser Doppler velocimetry; BET, Brunauer-Emmett-Teller; AAS, atomic absorption spectrophotometry; MNT, micronucleus test; CA assay, chromosomal aberration assay; ANOVA, analysis of variance; MN-PCEs, micronucleated polychromatic erythrocytes; PCEs, polychromatic erythrocytes; MI, mitotic index; TA, total aberrations; ROS, Reactive oxygen species; RES, reticuloendothelial system; MPS, mononuclear phagocytic system; BBB, blood brain barrier.

* Corresponding author. Fax: +91 40 27193227.
E-mail addresses: paramgrover@gmail.com, grover@iict.res.in (P. Grover).

0041-008X/$ – see front matter © 2012 Elsevier Inc. All rights reserved.
http://dx.doi.org/10.1016/j.taap.2012.10.016

lymphnodes, to provide information on tumour angiogenesis, to differentiate dangerous atherosclerosis plaques as well as healthy and pathological tissues (Hafeli et al., 2009). Additionally, trans gene expression can be viewed non invasively by MRI. *In vivo* apoptosis also can be detected by MRI with the help of nano scale Fe_2O_3 (Gupta and Gupta, 2005). Fe_2O_3 nanoparticles have been used for inducing magnetic hyperthermia, one of the therapies for cancer treatment which bears the exposition of cancer tissues to an alternating magnetic field (Gonzales-Weimuller et al., 2009). More over Fe_2O_3 NMs have also been developed as carriers for targeted drug delivery for treatment of various type of cancers, as cellular therapy such as cell labelling, targeting and as a tool for cell biology research to separate and purify cell populations (Xie et al., 2009). In addition nano sized Fe_2O_3 have found application in tissue repair through welding or through soldering (Lobel et al., 2000). Further, a promising method for gene delivery by Fe_2O_3 NMs is magnetofection which is defined as enhanced delivery of nucleic acids that are associated with NMs in to cells under the influence of external magnetic field (Scherer et al., 2002).

Even though nano scale Fe_2O_3 are very important commercially, the toxicity hazards associated with them are still unknown. A few studies have revealed that Fe_2O_3 NMs are toxic both *in vitro* and *in vivo*. A study showed that exposure of Fe_2O_3 nanoparticles to PC12 cells adversely affected cell functions (Pisanic et al., 2007).

Interactions of Fe_2O_3 NMs and murine macrophage (J774) cells at high concentration and prolonged exposure reduced viability using MTT assay. Necrosis-apoptosis assay demonstrated maximum loss of cells indicating apoptosis. H_2DCFDDA assay revealed that exposure to higher concentrations (300–500 ug/ml) resulted in reactive oxygen species (ROS) causing cell injury and death (Naqvi et al., 2010).

Fe_2O_3 nanoparticles have shown acute inhalation toxicity in rats treated with 8.5 mg/kg body weight (bw) of the compound (Wang et al., 2010b). Size dependent toxicological effects of Fe_2O_3 NMs was studied after 1, 7 and 30 days of intratracheal instillation in rats. Both the nano and sub-micron sized particles induced lung injury (Zhu et al., 2008). Translocation and interaction of Fe_2O_3 particles with nervous system was observed in intranasal instilled mice brain (Wang et al., 2007).

Worries over hazards of various diseases and cancer induction are worldwide. Hence genotoxicity is an important parameter of toxicity profiles of chemicals. Fe_2O_3 nanoparticles induced DNA-breakage in IMR-90 and BEAS-2B cells using comet assay indicating that it was clastogenic (Bhattacharya et al., 2009). The capacity of Fe_2O_3 NMs to induce DNA damage was evaluated after exposure to A549 cell line. The Fe_2O_3 nanoparticles showed slight toxicity by comet assay (Karlsson et al., 2009). Genotoxicity study with nano and micro scale particles of Fe_2O_3 by using comet assay showed slightly more potential to cause genotoxicity as compared to the bulk counterparts with BEAS-2B cells (Bhattacharya et al., 2012). On the other hand genotoxicity of nanoscale and bulk Fe_2O_3 did not show significant DNA damage using comet assay in Syrian hamster embryo cells (Guichard et al., 2012).

Studies that have examined the *in vivo* genotoxicity of NMs of Fe_2O_3 are not available. This prompted us to conduct an investigation on the genotoxicity of nano sized of iron oxide (Fe_2O_3-30 nm) and bulk (Fe_2O_3-bulk) using comet assay, micronucleus test (MNT) and chromosomal aberration (CA) assay in female rats using oral route. As far as we are aware the genotoxicity and biodistribution of Fe_2O_3 NMs in rats by oral route has not been carried out till date. Further, the gastrointestinal region is one of the most important portal of entry of NMs in humans and animals, hence the oral route was used for the current study (Oberdörster et al., 2005).

The comet assay is a sensitive method for the detection of DNA strand breaks and alkali-labile sites in individual cells, induced by a variety of genotoxic agents (Singh et al., 1988). The technique can also be adapted for the quantification of alkali-labile sites, oxidative base damage, DNA-DNA or DNA-protein cross-linking and abasic sites (Collins et al., 2008). The MNT determines the clastogenicity and the aneugenicity of compounds. In this assay rats peripheral blood cells can be collected without sacrificing the animals (Celik et al., 2005). The bone marrow MNT and CA assay are the most common genotoxicity screening tests. The MNT detects clastogenicity because of chromosome breakage due to chromosome lagging resulting from dysfunction of mitotic apparatus. CAs are due to failure in repair processes such that breaks either do not rejoin or rejoin in abnormal configurations.

Biodistribution study of NMs are essential to understand the amount of nanoparticles that enter in the target tissue or site. Targeted NMs should be transported from circulating blood to the tissues of interest and bind to its molecular target as a first step in nanoparticle retention or cellular internalization. Numerous NMs are hastily cleared from blood stream by reticulo endothelial system (RES) and the mononuclear phagocytic system (MPS) mainly through the liver, spleen and bone marrow (Peer et al., 2007; Ferrari, 2005). The *in vivo* metabolic processes of iron oxide NMs within the organism, as well as their distribution in the important organ tissues, are not yet completely understood (Powers et al., 2007). In this study the biodistribution of Fe_2O_3-30 nm and Fe_2O_3-bulk in rat's whole blood, liver, kidney, heart, brain, spleen, bone barrow, urine and feces was analyzed by using atomic absorption spectrophotometry.

It has become evident that the systematic and ample characterisation of NMs is important in order to understand their potential toxicity to biological systems (Murdock et al., 2008). Hence in the current investigation, the physicochemical properties of Fe_2O_3-30 nm and its bulk were determined by using transmission electron microscopy (TEM), dynamic light scattering (DLS), laser Doppler velocimetry (LDV) and surface area (Brunauer-Emmett-Teller) analysis. Further, the rationale of the present study was to assess the probable size, dose and time related acute genotoxic effects of Fe_2O_3-30 nm and Fe_2O_3-bulk by using comet, MNT and CA in whole blood cells and bone marrow cells of rats.

2. Materials and methods

2.1. Materials. All chemicals were purchased from Sigma Aldrich Inc., USA. However, phosphate-buffered saline (PBS) was obtained from Invitrogen, USA.

2.2. Nano and bulk particles of Fe_2O_3. Fe_2O_3-bulk materials size of <5 μm [CAT number 310050, purity ≥ 99%]& Fe_2O_3 nanopowder size of <50 nm [CAT number 544884, size, purity ≥ 98.1%] according to the manufacture's report were purchased from Sigma Aldrich Inc., USA. As per the manufacturer, the Fe_2O_3 NMs were synthesized via the thermal decomposition of Fe $(CO)_5$ in the presence of oleylamine (Peng et al., 2006).

2.3. Characterization. The NMs were characterized using TEM, DLS, LDV and ICP-MS to evaluate material size, size distribution, state of dispersion, zeta potential and purity of NMs in the solution respectively. Specific surface area analysis was determined by Brunauer-Emmett-Teller (BET) technique.

2.4. Transmission electron microscopy of Fe_2O_3 nano and bulk particles. TEM images of Fe_2O_3 NMs and its bulk were taken to obtain size and morphology on a TEM from JEOL, JEM-2100, Japan at an accelerating voltage of 200 kV. This has a plunge freezer along with cryo transfer holder to fix specimens in the frozen state and fitted with a Gatan 2 K × 2 K CCD camera for acquiring high-resolution images. Materials were suspended in water (1 mg/ml) and consequently one drop of suspension was placed on a carbon-coated copper TEM grids and allowed the solvent to evaporate at room temperature. The NMs were examined by using AMT Advanced Microscopy Techniques (AMT) software for the digital TEM camera calibrated for NM size measurement. For the size measurement 100 particles were calculated from random fields of view in addition to images that show general morphology of the NMs.

2.5. Dynamic light scattering and laser Doppler velocimetry of Fe_2O_3 nanomaterials in solution. The size of the NMs and agglomerates in solution were measured by DLS and LDV using a Malvern Instruments Zetasizer Nano-ZS Instrument. The device uses a 4 mW He-Ne 633 nm laser to analyze the samples as well as electric field generator for laser Doppler velocimetry measurements. The 50 ppm of freshly prepared Fe_2O_3 NMs suspension in Milli Q water was ultra sonicated using probe sonicator (UPH 100, Germany) for 10 min. Since, the concentration was too high hence, it was further diluted, adjusted to a lower concentration, for the device to acquire enough counts per second. The prepared samples were transferred to a 1.5 ml square cuvette for DLS measurements and 1 ml was transferred to a Malvern Clear Zeta Potential cell for LDV measurement. The mean NMs diameter was calculated by the software from the NMs distributions measured and the polydispersity index (PdI) given was a measure of the size ranges present in the solution. The PdI scale ranges from 0 to 1, with 0 being monodisperse and 1 being polydisperse.

2.6. Surface area analysis. The specific surface areas (m^2/g) of the Fe_2O_3-30 nm and Fe_2O_3-bulk particles were measured by N_2 adsorption–desorption measurement at 77 K by the Brunauer–Emmett–Teller (BET) method using a surface area analyzer Quadrusorb-SI V 5.06 instrument (M/S Quanta chrome Instruments Corporation, USA).

2.7. Purity analysis. The ICP-MS analysis was performed for the purity of the Fe_2O_3 compounds according to the method given by Yokel et al., 2009. The results showed the presence of $<1.3\%$ other impurity in Fe_2O_3 bulk and $<2.0\%$ of other contamination in Fe_2O_3 nanomaterials. Hence the purity of Fe_2O_3 NMs was $>98\%$ and of Fe_2O_3 bulk was $>98.7\%$.

2.8. Animals. Albino Wistar female rats aged 6–8 weeks and weighing 80–120 g were obtained from National Institute of Nutrition, Hyderabad, India. The animals were housed for a week for acclimatisation in groups of five in standard polypropylene cages with stainless steel top grill. Clean paddy husk was used as a bedding material. The animals were fed on commercial pellet diet and water *ad libitum* in polypropylene bottles with stainless steel sipper tubes. The animals were maintained under standard conditions of humidity (55-65%), temperature (22 ± 3 °C) and light (12 h light/ 12 h dark cycles). The study was approved by Institutional Animal Ethical Committee of IICT, India.

2.9. Acute oral treatment. The study was designed in accordance with the method provided by Organization for Economic Cooperation and development (OECD) namely "Acute oral toxicity-fixed dose method" (OECD, 2001). Before treatment, animals were fasted overnight. The Fe_2O_3-30 nm and Fe_2O_3-bulk were suspended in deionised water. A single rat was dosed first with 5 mg/kg bw dose. If no mortality and symptoms were found, the second rat received 50 mg/kg bw dose, then 300 mg/kg bw and finally, 2000 mg/kg bw dose in sequence in the sighting study. Since no mortality and toxic symptoms were found at any dose level in the sighting study, the main study with five rats was done at 2000 mg/kg bw dose level for Fe_2O_3-30 nm and Fe_2O_3-bulk. Since the acute toxicity of test compounds was greater than 2000 mg/kg bw. Therefore, three dose levels of Fe_2O_3-30 nm and Fe_2O_3-bulk: 500, 1000, 2000 mg/kg bw were used for the genotoxicity studies and biodistribution (Kumari et al., in press).

2.10. Experimental design. The rats were randomly divided into three groups: the positive control, the control and the experimental groups. The experimental groups were again divided into three subgroups based on the acute toxicity data. Therefore, three dose levels of Fe_2O_3-30 nm and Fe_2O_3-bulk: 500, 1000, 2000 mg/kg bw were used for the genotoxicity studies and biodistribution. All groups had the same number of animals per test. Thus, for comet assay/blood MNT, bone marrow MNT and CA assay, five rats each were used per group per sampling time. Doses of the experimental groups were obtained by suspending 500, 1000, 2000 mg/kg bw of Fe_2O_3-30 nm and Fe_2O_3-bulk in Milli Q water after sonication using a probe sonicator (UPH 100, Germany) for 10 min. The control groups were treated with 5 ml/kg bw of Milli Q water and experimental groups were treated with Fe_2O_3-30 nm and Fe_2O_3-bulk (500, 1000, 2000 mg/kg bw) by oral gavage. Cyclophosphamide, a known mutagen, was used as the positive control at a dose 40 mg/kg bw. It was given intraperitonially (i.p.) and the volume injected was 0.01 ml/g bw. All rats received a single dose and all the treated rats were sacrificed by cervical dislocation at specific sampling time.

2.11. Comet assay. The alkaline comet assay was conducted for the assessment of DNA damage following the guidelines proposed by (Singh et al., 1988, Tice et al., 2000) with slight modifications. Three slides were prepared for each experimental point. Cell viability was determined by trypan blue exclusion assay (Pool-Zobel et al., 1994). The peripheral blood was collected at 6, 24, 48 and 72 h after the dosing. The microscope slides were coated with 0.75% normal-melting-point agarose (NMPA) in PBS, 20 μl of heparinised peripheral blood was mixed with 110 μl of 0.5% low-melting-point agarose (LMPA) in phosphate buffered saline (PBS) and applied to slides. The slides were covered with a cover slip and refrigerated for 5 min to solidified the gel. The cover slips were removed and slides were immersed for at least 1 h in ice-cold alkaline lysing solution [2.5 M NaCl, 10 mM Tris, 100 mM ethylenediaminetetraacetic acid (EDTA), 10% dimethyl sulphoxide, 1% Triton X-100] at final pH 10.0. After that slides were incubated in ice-cold electrophoresis solution (0.3 M NaOH, 1 mM EDTA, pH > 13) for 20 mins, followed by electrophoresis at 25 V : 300 mA (1.25 V/cm) for 25 min. After electrophoresis, the slides were neutralized with neutralizing buffer (Tris 0.4 M, pH 7.5) and then stained with ethidium bromide (20 μg/ml). One hundred cells per rat (50 cells analysed in each slide) were scored at 400× using a fluorescence microscope (Olympus-Japan) with a blue (488 nm) excitation filter and yellow (515 nm) emission (barrier) filter. One scorer analysed the slides throughout the study and all the slides were coded. Detection of DNA breakage was measured by using a Comet Image Analysis System, version 6 (Kinetic Imaging Ltd, Nottingham, UK). The % tail DNA damage was used to evaluate DNA damage (Lovell and Omori, 2008).

2.12. Peripheral blood Micronucleus test. The peripheral blood micronucleus test was conducted according to the OECD guidelines 474 (OECD, 1997a) and the protocol described by (Celik et al., 2005) in the peripheral blood cells of albino Wistar rats. After 48 and 72 h of treatment peripheral blood cells were collected and smears were prepared on microscope slides with cells, air dried, fixed in methanol and stained with 0.04 mM acridine orange solution in pH 6.8 phosphate buffer. The MNT analysis was done with a fluorescence microscope (Olympus-Japan) using a 100× objective. The number of micronucleated polychromatic erythrocytes (MN-PCEs) among 2000 PCEs per animal were examined. The quantity of polychromatic erythrocytes (PCEs) per total erythrocytes was determined from a total of 1000 erythrocytes per rat.

2.13. Bone marrow micronucleus test. The mammalian *in vivo* micronucleus test is widely used for the detection of cytogenetic damage with test substance. For the MN analysis, method described by (Schmid, 1975) was used in polychromatic erythrocytes (PCEs) of rats bone marrow cells extracted from thigh bone. The femurs were removed, the bone marrow was collected, centrifuged, spread on the slides and allowed to dry in humidified air overnight. The slides were fixed with methanol and stained with Giemsa (Sigma Chemical Co., St. Louis, MO) solution in phosphate buffer saline for the assessment of the micronuclei (MN) occurrence. The study was done at 24 and 48 h of after treatment according to OECD Guideline 474 (OECD, 1997a). Three slides were made for each animal; the slides were microscopically analyzed at 1000× magnification. Per animal, 2000 PCEs were randomly selected from three slides and scored for the presence of MN.

Table 1
Characteristics of Fe_2O_3 nanomaterials and Fe_2O_3-bulk.

Nanomaterial	Size using TEM	DLS		LDV			Surface area (m^2/g)
		Average diameter	PDI (nms)	Zeta potential ζ (mV)	Electrophoretic mobility μ (μm cm/V/s)	pH	
Fe_2O_3 NMs	29.75 ± 1.87(nm)	363	0.406	−18.6	−1.47	−7.0	38.02
Fe_2O_3 bulk	2.13 ± 4.15(μm)	-	-	-	-	7.0	5.76

Fe_2O_3 nanomaterial and its bulk were dispersed in MilliQ water, mixing was done via probe sonication for 10 min.

2.14. Chromosomal aberration assay. CA analysis was done by the method of rinsing rat's bone marrow cells (femur and tibia) as described previously (Adler, 1984). The bone marrow was collected and centrifuged. Cells were then fixed through several changes of ice-cold methanol/glacial acetic acid (3:1, v/v) until the pellets were clean. After refrigeration for at least 24 h, cells were centrifuged and resuspended in fresh fixative, dropped onto slides, dried and stained with Geimsa. Three slides for each animal were made by the flame-dried technique. CAs were identified on the basis of criteria established by the OECD Guideline 475 (OECD, 1997b). The analysis was carried out at two sampling of 18 and 24 h. Five hundred well spread metaphases were selected to detect the presence of CAs; while the mitotic index (MI) was determined with 1000 or more cells at both the sampling times.

2.15. Sample collection and preparation for the detection of iron (Fe) content in different organs, urine and feces. To collect the samples for biodistribution the animals were placed in metabolic cages after treatment. Urine and feces samples were collected and pooled at 0-6 h, 6-24 h, 24-48 h, and 48-72 h after the dosing. Whole blood, liver, kidneys, heart, brain, spleen and bone marrow cells were taken out after sacrifice of rats at 6 h, 24 h, 48 h, and 72 h. Bone marrow was extracted by flushing the bone marrow cavity with phosphate-buffered saline (PBS) then centrifuged to pellet the marrow. Prior to elemental analysis approximately ~0.3 g of fresh liver, kidneys, heart, brain, spleen, feces and ~0.3 ml of blood and urine samples were taken from the treated rats after a single dose of 500, 1000, 2000 mg/kg bw of Fe_2O_3-30 nm and Fe_2O_3-bulk. They were pre-digested in nitric acid for overnight. Samples were then heated at 80 °C for 10 h followed by additional heating at 130–150 °C for 30 min. Finally, in the presence of 0.5 ml of 70% perchloric acid, the samples were again heated for 4 h, and evaporated nearly to dryness (Wang et al., 2010a). Following digestion, samples were filtered and made up to 25 ml using milli Q water for analysis.

The Fe content in the samples was determined by using atomic absorption spectrophotometry. Blank levels were found to be below detection limits in all cases.

2.16. Statistical analysis. The statistical significant change in genotoxicity assays and biodistribution study between treated and control groups were analyzed by one-way ANOVA. Results were expressed as mean ± standard error (S.E.). Multiple comparisons were performed by Tukey's test. All calculations were performed using Graph Pad Prism 4 Software package for windows. The statistical significance for all tests was set at $p<0.05$.

3. Results

3.1. Nanomaterials characterization

The result of Fe_2O_3 NMs characterisation estimated by TEM, measured by BET analysis, determined by zeta potential and electrophoretic mobility, DLS and LDV data obtained are shown in Table 1.

The particle size and appearance of the Fe_2O_3 NMs and its bulk were determined by TEM images (Figs. 1 and 2) and showed spherical morphology. The mean size distribution of Fe_2O_3 NMs and Fe_2O_3 bulk was 29.75 nm and 2.15 μm respectively. The DLS value for Fe_2O_3 NMs size in Milli Q water suspension was 363 nm. The result of DLS showed larger values than NMs size measured by TEM, indicating that Fe_2O_3-30 nm NMs formed larger agglomerates in suspension. Zeta potential and electrophoretic mobility measurements were −18.6 mV and −1.47 μ (μm cm/V/s) respectively at pH 7.0. DLS and LDV data was found to be out of detection limit, in the case of bulk material. The specific surface area of Fe_2O_3 NMs and Fe_2O_3 bulk determined by BET analysis was 38.02 and 5.67(m^2/g) respectively.

3.2. Comet assay

The results obtained by comet assay after acute oral treatment with Fe_2O_3-30 nm and Fe_2O_3-bulk materials are summarized in Table 2. In all experiments the cell viability by the trypan blue exclusion technique ranged from >90% (data not shown). In rats treated orally with 500,

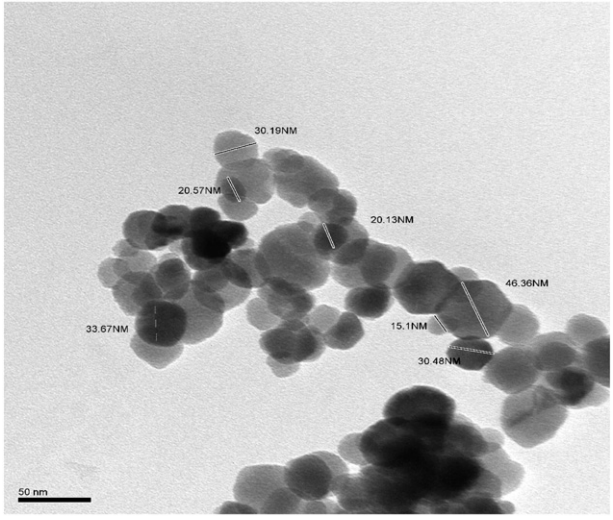

Fig. 1. TEM image for Fe_2O_3-30 nm suspension in water.

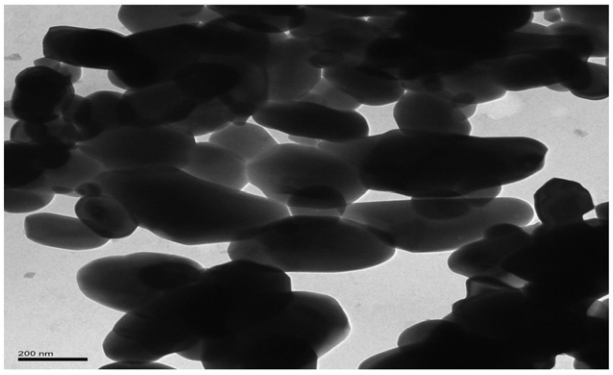

Fig. 2. TEM image for Fe_2O_3-bulk suspension in water.

Table 2
Mean % tail DNA in peripheral blood leucocytes of female Wistar rats exposed orally to different doses of Fe_2O_3-30 nm and Fe_2O_3-bulk at 6, 24, 48 and 72 h.

Treatments	Dose (mg/kg bw)	Sampling times (h)			
		6 h	24 h	48 h	72 h
Control[a]		3.82 ± 0.77	5.44 ± 0.81	4.17 ± 0.80	4.36 ± 0.92
Fe_2O_3 30 nm	500	3.26 ± 0.51	5.32 ± 0.90	4.18 ± 0.76	4.24 ± 0.60
	1000	3.84 ± 0.66	5.59 ± 1.02	4.52 ± 0.72	4.32 ± 0.67
	2000	4.14 ± 0.86	6.01 ± 0.97	5.06 ± 1.01	4.62 ± 0.80
Fe_2O_3-bulk	500	3.77 ± 0.47	4.81 ± 59	4.08 ± 0.67	3.46 ± 0.47
	1000	3.99 ± 0.81	5.28 ± 0.70	4.30 ± 0.75	4.15 ± 0.85
	2000	4.01 ± 0.69	5.61 ± 0.86	4.59 ± 0.88	4.29 ± 0.77
CP[b]	40	43.94 ± 6.50[c]	54.56 ± 6.31[c]	25.39 ± 4.65[c]	16.10 ± 2.21[c]

[a]Deionised water (negative control), [b]Cyclophosphamide (positive control), Data represented as mean ± S.E., of 3 replicated experiments, 150 cells per animal, n = 5 animals, significantly different from control at Significantly different from control at c = p<0.001.

1000 and 2000 mg/kg of Fe_2O_3-30 nm and Fe_2O_3-bulk, no statistically significant damage was observed at 6, 24, 48, 72 h sampling time in comparison to control ($p > 0.05$). In the present study, an intraperitoneal injection of CP (40 mg/kg) induced DNA damage in rat peripheral blood leukocytes. The mean % tail DNA was significantly ($p < 0.001$) higher compared to control.

3.3. Peripheral blood micronucleus test

The results from blood MNT are shown in Table 3. The % of PCEs in Fe_2O_3-30 nm and Fe_2O_3-bulk treated groups of animals were not reduced at various doses (500, 1000, 2000 mg/kg bw). The animal groups sampled at 48 and 72 h after treatment with various doses of Fe_2O_3-30 nm and Fe_2O_3-bulk fell well within normal control ranges and did not show significant difference ($p > 0.05$) from control. The data reveals that the compounds did not cause cytotoxicity. The MN-PCEs calculated after treatment with all the three doses of Fe_2O_3-30 nm and Fe_2O_3-bulk did not show statistically significant differences ($p > 0.05$) as compared to control at both the sampling times suggesting lack of clastogenicity. CP treated group showed significant difference ($p < 0.001$) with respect to the control group.

3.4. Bone marrow micronucleus test

The bone marrow MNT was determined after 24 h and 48 h of oral administration of Fe_2O_3-30 nm and Fe_2O_3-bulk at various doses (500, 1000, 2000 mg/kg bw) in female albino wistar rats (Table 4). The MN-PCEs frequencies in the Fe_2O_3-30 nm and Fe_2O_3-bulk treated groups were very similar to those in controls and were not significantly different ($p > 0.05$). On the other hand, CP (40 mg/kg bw) treated positive control groups induced a substantially significant ($p < 0.001$) effect on MN-PCEs frequency.

In the MNT with varied doses of Fe_2O_3-30 nm and Fe_2O_3-bulk materials exhibited no statistically difference in % PCEs with the negative control at 24 and 48 h after treatment, demonstrating the absence of bone marrow cytotoxicity.

3.5. Chromosomal aberrations

Tables 5 and 6 shows the CA assay results obtained with Fe_2O_3-30 nm and Fe_2O_3-bulk bone-marrow cells of rats at 18 h and 24 h. The MI did not reveal any statistical differences ($p > 0.05$) between the various treatments (2000 mg/kg, 1000 mg/kg and 500 mg/kg of Fe_2O_3 30 nm and its bulk) and control groups. The Fe_2O_3-30 nm and Fe_2O_3-bulk did not induce a dose dependent effect on the structural (gaps, breaks, minute, acentric fragment and reciprocal translocation) and numerical (aneuploidy and polyploidy) CAs as well as percentage (%) of aberrant cells at all the doses and treatment times.

The total cytogenetic changes (numerical + structural CAs), total aberrations (structural aberrations) including and excluding gaps frequencies in Fe_2O_3-30 nm and Fe_2O_3-bulk were well within normal control range, and were not significantly different ($p > 0.05$) from concurrent controls.

3.6. Bio distribution of Fe and composition changes in organs, urine and feces

The distribution of Fe in the various organs, tissues, urine and feces of rats is shown in Fig. 3. Fe accumulated in all the tissues viz., whole blood, liver, heart, kidneys, bone marrow and spleen in the groups of animals treated with Fe_2O_3-30 nm. After reaching the highest level at different time points in different organs, a gradual decrease was found in the Fe level in all the organs. The maximum amount of Fe was found in liver, kidney and blood at 24 h, then gradually decreased at 72 h. In the bone marrow cells and heart the highest Fe level was detected at 48 h. However, subsequently decline was found in Fe at

Table 3
Frequency of MN-PCEs and % PCEs in peripheral blood leucocytes treated orally with different doses of Fe_2O_3-30 nm and Fe_2O_3-bulk at 48 h and 72 h.

Treatments	Dose (mg/kg bw)	48 h h		72 h	
		MN-PCEs	%PCEs	MN-PCEs	%PCEs
Control[a]		1.4 ± 0.51	3.98	1.2 ± 0.37	3.34
Fe_2O_3-30 nm	500	1.2 ± 0.20	3.79	1.2 ± 0.58	3.13
	1000	1.6 ± 0.68	3.84	1.4 ± 0.60	3.26
	2000	2.2 ± 0.66	3.60	2.0 ± 0.71	3.03
Fe_2O_3-bulk	500	1.2 ± 0.49	3.58	1.0 ± 0.45	3.19
	1000	1.4 ± 0.50	3.72	1.2 ± 0.20	3.24
	2000	1.8 ± 0.58	3.81	1.6 ± 0.51	3.36
CP[b]	40	30.8 ± 3.98[c]	1.40	24.6 ± 3.36[c]	2.03

[a]Deionised water (negative control). [b]Cyclophosphamide (positive control), Data represented as mean ± S.E., Significantly different from control at Significantly different from control at c = p<0.001, n = 5 animals per group.

Table 4
Frequency of MN-PCEs and % PCEs in female Wistar rat bone marrow cells treated orally with different doses of Fe_2O_3-30 nm and Fe_2O_3-bulk at 24 h and 48 h.

Treatments	Dose (mg/kg bw)	24 h		48 h	
		MN-PCEs	%PCEs	MN-PCEs	%PCEs
Control[a]		2.0 ± 0.92	44.00	2.2 ± 0.86	42.20
Fe_2O_3-30 nm	500	2.2 ± 0.73	44.10	2.0 ± 0.45	43.70
	1000	2.6 ± 0.67	43.60	2.4 ± 0.60	44.30
	2000	3.0 ± 0.89	42.70	2.6 ± 0.93	42.00
Fe_2O_3-bulk	500	1.8 ± 0.37	44.90	2.0 ± 0.71	43.10
	1000	2.0 ± 0.31	42.80	2.2 ± 0.58	43.40
	2000	2.4 ± 0.51	42.50	2.6 ± 0.74	43.00
CP[b]	40	34.4 ± 2.96[c]	28.40	34.0 ± 3.72[c]	28.00

[a]Deionised water (negative control). [b]Cyclophosphamide (positive control), Data represented as mean ± S.E., Significantly different from control at Significantly different from control at c = p<0.001, n = 5 animals per group.

Table 5
Chromosome aberrations and % mitotic index observed in bone-marrow cells of female Wistar rats treated with different doses of Fe_2O_3-30 nm and Fe_2O_3-bulk at 18 h.

Dose (mg/kg b.w.)	M.I. (%) M ± SE	Chromosomal aberrations							Aberrant cells (%)	Total cytogenetic changes	TA + gaps M ± SE	TA-gaps M ± SE
		Numerical aberrations		Structural aberrations								
		Aneuploidy	Polyploidy	Gaps	Breaks	Minute	Acentric Fragments	Reciprocal translocations				
Con.[a]	3.20 ± 0.21	0.8 ± 0.4	0.0 ± 0.0	0.8 ± 0.4	0.4 ± 0.2	0.2 ± 0.2	0.2 ± 0.0	0.00 ± 00	0.6 ± 0.24	2.4 ± 0.8	1.6 ± 0.5	0.8 ± 0.20
Fe_2O_3-30 nm												
500	3.25 ± 0.18	0.6 ± 0.4	0.0 ± 0.0	0.4 ± 0.4	0.2 ± 0.2	0.4 ± 0.2	0.2 ± 0.2	0.0 ± 00	0.6 ± 0.40	1.8 ± 0.6	1.2 ± 0.5	0.8 ± 0.24
1000	3.05 ± 0.21	0.8 ± 0.4	0.0 ± 0.0	0.6 ± 0.4	0.4 ± 0.2	0.4 ± 0.2	0.2 ± 0.2	0.0 ± 00	0.8 ± 0.37	2.4 ± 0.8	1.6 ± 0.5	1.0 ± 0.45
2000	3.15 ± 0.20	0.8 ± 0.5	0.0 ± 0.0	0.8 ± 0.5	0.4 ± 0.2	0.6 ± 0.4	0.4 ± 0.2	0.0 ± 00	1.0 ± 0.45	3.0 ± 1.0	2.2 ± 0.8	1.4 ± 0.40
Fe_2O_3-bulk												
500	3.20 ± 0.21	0.6 ± 0.4	0.0 ± 0.0	0.4 ± 0.4	0.2 ± 0.2	0.2 ± 0.2	0.2 ± 0.2	0.0 ± 0.0	0.4 ± 0.24	1.6 ± 0.7	1.0 ± 0.77	0.6 ± 0.40
1000	3.15 ± 0.20	0.8 ± 0.4	0.0 ± 0.0	0.4 ± 0.2	0.4 ± 0.2	0.2 ± 0.2	0.2 ± 0.2	0.0 ± 0.0	0.6 ± 0.40	2.0 ± 0.5	1.2 ± 0.68	0.8 ± 0.58
2000	3.03 ± 0.21	0.8 ± 0.4	0.0 ± 0.0	0.6 ± 0.4	0.4 ± 0.4	0.4 ± 0.2	0.4 ± 0.2	0.0 ± 0.0	0.6 ± 0.40	2.6 ± 0.9	1.8 ± 0.89	1.2 ± 0.73
CP[b]	1.88 ± 0.18	38.4 ± 1.8[c]	3.4 ± 0.5[c]	12.2 ± 1.6[c]	10.4 ± 1.3[c]	11.6 ± 1.9[c]	13 ± 1.2[c]	1.8 ± 0.5 [c]	37 ± 1.41[c]	90.8 ± 5.4[c]	49 ± 3.61[c]	36.8 ± 3.51[c]

Significantly different from control at $c = p < 0.001$. One hundred metaphases were analyzed per animal; n = 5 animals per group.
Total cytogenetic changes = numerical aberrations and structural aberrations. % aberrant cells correspond to cells with ≥1 aberration excluding gaps. MI, mitotic index; data represented as mean ± standard error; TA, total aberrations = structural aberrations. [a]Negative control – deionised water. [b]Cyclophosphamide (40 mg/kg).

72 h. Spleen showed the high accumulation of Fe at 72 h with all three doses of Fe_2O_3 -30 nm. In this study, no significant increase was observed in brain Fe levels after the treatment of Fe_2O_3-30 nm as well as Fe_2O_3-bulk at all the doses tested. The Fe_2O_3-bulk treated groups did not show statistically significant biodistribution of Fe in kidneys, heart, blood and urine as compared to control. Nevertheless, it showed significant Fe accumulation in liver after 24 and 48 h with the dose of 2000, 1000 mg/kg bw and 2000 mg/kg bw respectively. In spleen significant Fe distribution was found at 72 h with 2000 mg/kg bw treated with Fe_2O_3-bulk. In the bone marrow cells after 24 and 48 h the significant increase was found only with 2000 mg/kg bw. By comparing the concentration of Fe at all time points between the experimental and control groups, more accumulation was in 2000 mg/kg bw followed by 1000 and 500 mg/kg bw of rats treated with Fe_2O_3-30 nm.

Further, we also found that the distribution of Fe in various organs, tissues was very high in NM treated groups as compared to bulk treated groups at all time points as well as dose levels. In the Fe_2O_3-30 nm, treated rats significant amount of Fe was removed via urine at all the time points and doses, more excretion of Fe was found with 2000 mg/kg bw followed by in the decreasing order in 1000 mg/kg bw, 500 mg/kg bw. In contrast, Fe_2O_3–bulk treated rats showed large excretion in feces. Clearance of Fe in feces decreased at an extremely fast speed from 24 to 72 h and from 2000 mg/kg bw to 1000 mg/kg bw, 500 mg/kg bw of doses. Therefore urine showed higher level of Fe in NMs treated groups, where as bulk treated groups showed largest retention in feces at all the doses and sampling time.

4. Discussion

In the era of nanotechnology an increasing concern about the impact of NMs on human health is raised by public as well as government. There is an increased risk for exposure of workers as well as consumers and the general public and environment. Because of the very small size and large surface area, NMs are able to enter easily into the body via inhalation, dermal and oral routes. There are a number of direct and indirect mechanisms that can subsequently promote genotoxicity. As per our knowledge, this is the first genotoxicity and biodistribution study with Fe_2O_3-30 nm and Fe_2O_3-bulk by oral route in albino female Wistar rats and the aim of this study was to compare genotoxic ability and biodistribution of the Fe_2O_3-30 nm and its bulk by oral route in rats. The exposure and uptake of NMs can take place through different routes including oral route. Humans involved in the manufacturing of Fe_2O_3 NMs may be exposed by unintentional hand to mouth transfer of NMs. Further, if these NMs are accidently released into the environmental, via the food chain, they may enter the human body. Moreover, these NMs may be swallowed by accident and reach the gastrointestinal tract. Hence we used the oral route for the current study. Further, high doses were used to obtain genotoxicity if any and to provide detectable Fe levels after accumulation within the animal and were not intended to reflect likely human exposure.

The results of the present study showed that Fe_2O_3-30 nm and Fe_2O_3-bulk were not proficient to cause increase in % Tail DNA damage,

Table 6
Chromosome aberrations and % mitotic index observed in bone-marrow cells of female Wistar rats treated with different doses of Fe_2O_3-30 nm and Fe_2O_3-bulk at 24 h.

Dos Dose (mg/kg b.w.)	M.I. (%) M ± SE	Chromosomal aberrations							Aberrant Cells (%)	Total cytogenetic changes	TA + gaps M ± SE	TA-gaps M ± SE
		Numerical aberrations		Structural aberrations								
		Aneuploidy	Polyploidy	Gaps	Breaks	Minute	Acentric Fragments	Reciprocal translocations				
Con.[a]	3.10 ± 0.17	1.0 ± 0.5	0.0 ± 0.0	0.6 ± 0.2	0.4 ± 0.2	0.4 ± 0.4	0.2 ± 0.2	0.00 ± 00	0.6 ± 0.24	2.6 ± 0.81	1.6 ± 0.5	1.0 ± 0.32
$Fe_2O_3$30nm												
500	3.00 ± 0.28	0.6 ± 0.4	0.0 ± 0.0	0.6 ± 0.2	0.4 ± 0.4	0.2 ± 0.2	0.2 ± 0.2	0.00 ± 00	0.4 ± 0.40	2.0 ± 0.32	1.4 ± 0.4	0.8 ± 0.40
1000	3.25 ± 0.18	1.0 ± 0.5	0.0 ± 0.0	0.6 ± 0.4	0.6 ± 0.2	0.4 ± 0.2	0.2 ± 0.2	0.00 ± 00	0.6 ± 0.40	2.8 ± 0.58	1.8 ± 0.4	1.2 ± 0.20
2000	3.05 ± 0.21	1.0 ± 0.6	0.0 ± 0.0	0.8 ± 0.5	0.6 ± 0.4	0.4 ± 0.2	0.4 ± 0.4	0.00 ± 00	0.8 ± 0.37	3.2 ± 0.86	2.2 ± 0.7	1.4 ± 0.40
Fe_2O_3-bulk												
500	3.25 ± 0.18	0.4 ± 0.2	0.0 ± 0.0	0.4 ± 0.4	0.4 ± 0.2	0.2 ± 0.2	0.2 ± 0.2	0.0 ± 0.0	0.6 ± 0.40	1.6 ± 0.5	1.2 ± 0.5	0.8 ± 0.24
1000	3.00 ± 0.28	0.6 ± 0.4	0.0 ± 0.0	0.6 ± 0.4	0.6 ± 0.4	0.2 ± 0.2	0.2 ± 0.2	0.0 ± 0.0	0.4 ± 0.40	2.2 ± 0.6	1.6 ± 0.8	1.0 ± 0.55
2000	3.05 ± 0.21	0.8 ± 0.4	0.0 ± 0.0	0.6 ± 0.4	0.6 ± 0.4	0.4 ± 0.2	0.4 ± 0.2	0.0 ± 0.0	0.6 ± 0.40	2.8 ± 0.4	2.0 ± 0.5	1.4 ± 0.24
CP[b]	1.75 ± 0.20	41.4 ± 1.8[c]	4 ± 0.9[c]	13 ± 1.4[c]	11 ± 1.2[c]	12 ± 1.6[c]	13.4 ± 1.3[c]	2 ± 0.4[c]	38.6 ± 1.81[c]	96.8 ± 2.1[c]	51.4 ± 1.69[c]	38.4 ± 1.63[c]

Significantly different from control at $c = p < 0.001$. One hundred metaphases were analyzed per animal; n = 5 animals per group.
Total cytogenetic changes = numerical aberrations and structural aberrations. % aberrant cells correspond to cells with ≥1 aberration excluding gaps. MI, mitotic index; data represented as mean ± standard error; TA, total aberrations = structural aberrations.[a] Negative control – deionised water.[b] Cyclophosphamide (40 mg/kg).

micronucleus formation and chromosomal aberrations in comparison to control by the comet assay, MNT and CAs at all time intervals and doses tested. Similar *in vivo* genotoxicity studies with Fe_2O_3 NMs using comet assay have not been reported. However *in vitro* studies of Fe_2O_3 NMs with comet assay are available which are in accordance with our results. A549 cells treated with Fe_2O_3 nano and micrometer size particles showed low toxicity or no significant difference between the different particle sizes (Karlsson et al., 2009). 2,3-dimercaptosuccinic acid (DMSA) coated Fe_2O_3 nanoparticles showed genotoxicity only at concentration of 10–100 ug/ml with comet assay (Auffan et al., 2006).

Our study showed a lack of genotoxicity with MNT. Likewise Fe_2O_3 nanoparticles failed to induce significant increase in frequency of MN in mice bone marrow cells after acute treatment by intraperitoneal route (Wang et al., 2009). On the other hand an *in vivo* study of magnetite nanoparticles coated with polyaspartic acid, showed a time and dose dependent increased in MN-PCEs in Swiss mice after intravenous administration (Sadeghiani et al., 2005). Our study indicated that the % PCEs calculated in Fe_2O_3-30 nm and Fe_2O_3-bulk treated groups did not induce any significant decrease compared to the control group suggesting that cell death had not occurred in any of the treated groups.

The results of the bone marrow CA analysis with Fe_2O_3-30 nm as well as Fe_2O_3-bulk in rats indicated that these compounds were negative for induction of total CA including and excluding gaps as well as % aberrant cells in bone marrow. The percent MI suggested that Fe_2O_3-30 nm and Fe_2O_3-bulk were not cytotoxic. Our CA assay results are in

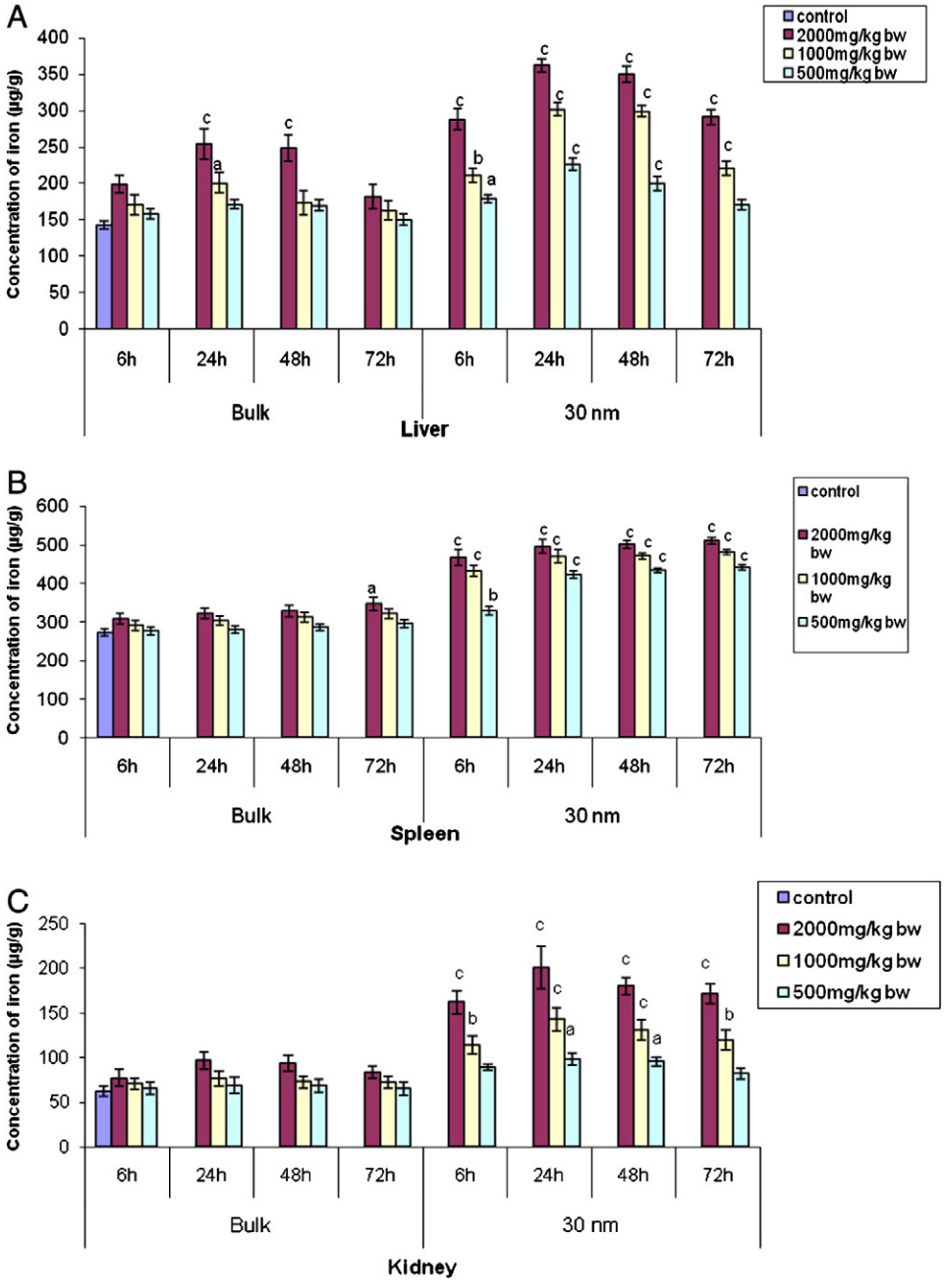

Fig. 3. Tissue distribution of Fe measured by AAS in A- Liver, B- Spleen, C- Kidney, D- Brain, E- Heart, F- Blood, G- Bone marrow, H- Urine, I- Feces of rats after single oral administration of 2000 mg/kg, 1000 mg/kg and 500 mg/kg bw of Fe_2O_3-30 nm and Fe_2O_3-bulk at 6, 24, 48 and 72 h of sampling time. Significantly different from control at a = $p<0.05$, b = $p<0.01$, c = $p<0.001$ by ANOVA followed by Tukey's test.

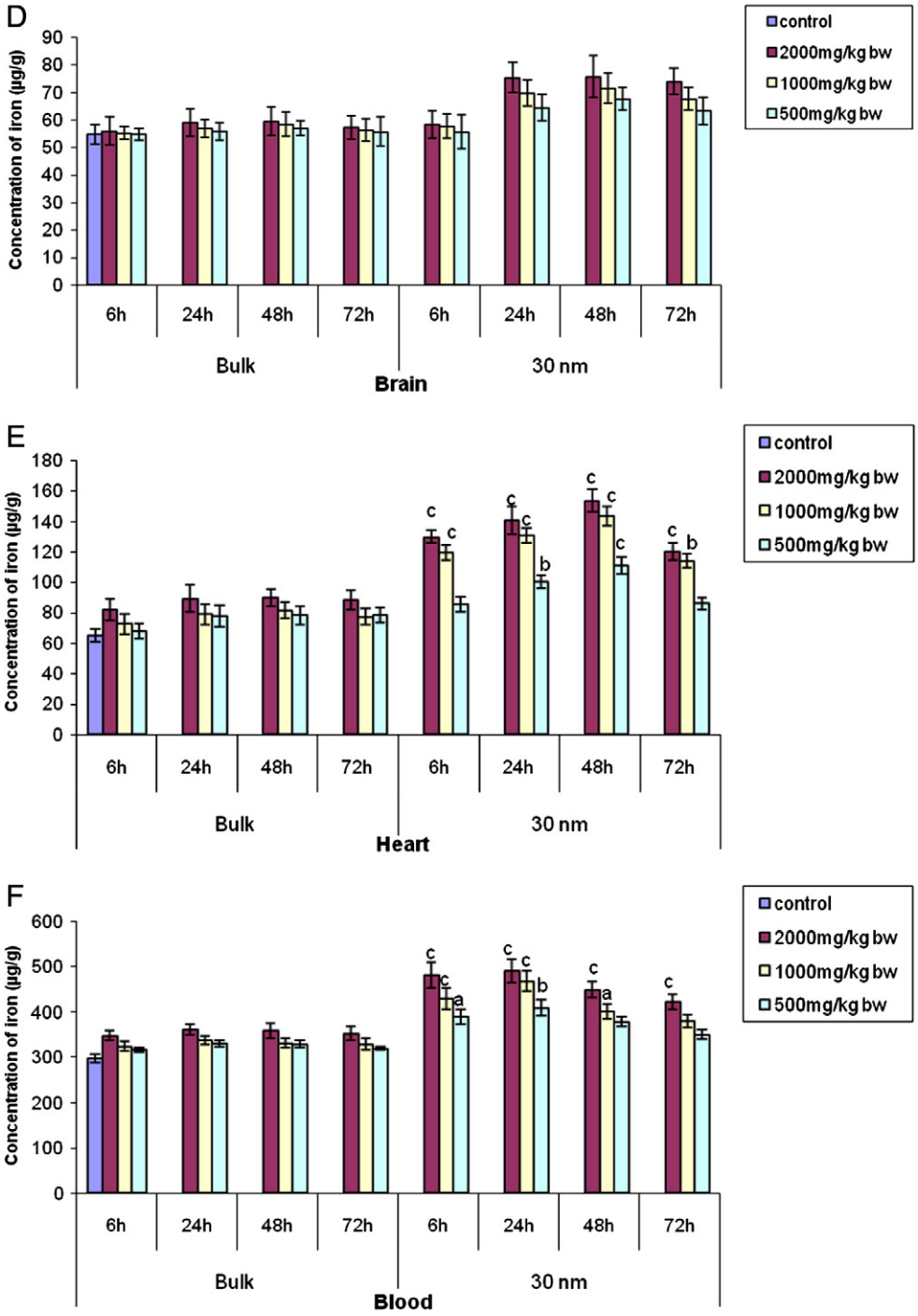

Fig. 3 (*continued*).

agreement with an investigation in Chinese hamster lung fibroblast cells with SiO_2 coated 50 nm MNPs (Kim et al., 2006). The result of this study did not show significant increase in CAs. The mechanism accountable for the genotoxicity of NMs implicates oxidative stress which cause redox imbalance with in cells usually as a result of increase in intracellular reactive oxygen species (ROS). ROS generated in the metabolizing cells could attack DNA base guanine and form 8-OHdG lesions, which are known to have mutagenic potential (Singh et al., 2009). A few studies have shown that significant oxidative DNA damage was not found as FPG-sites (% tail DNA) in A549 cells after 4 h exposure to 40 µg/cm^2 nano and micro particles of Fe_2O_3 at different compositions (Karlsson et al., 2009). Likewise when rats were exposed to iron particulate matter through inhalation, significant oxidative stress was not found (Zhou et al., 2003). Similarly, significant difference was not found in TiO_2-P25 and T805 instilled rat lung tissue as compared to control in amount of 8-oxoGua as a marker of DNA damage (Rehn et al., 2003). Fe_2O_3 nanoparticles did not cause protein oxidation in the cultured A549 human lung epithelial cells (Gua et al., 2009). These studies are in concurrence with our results. Different kinds of routes of exposure as well as *in vitro* and *in vivo* studies may shown different results with Fe_2O_3

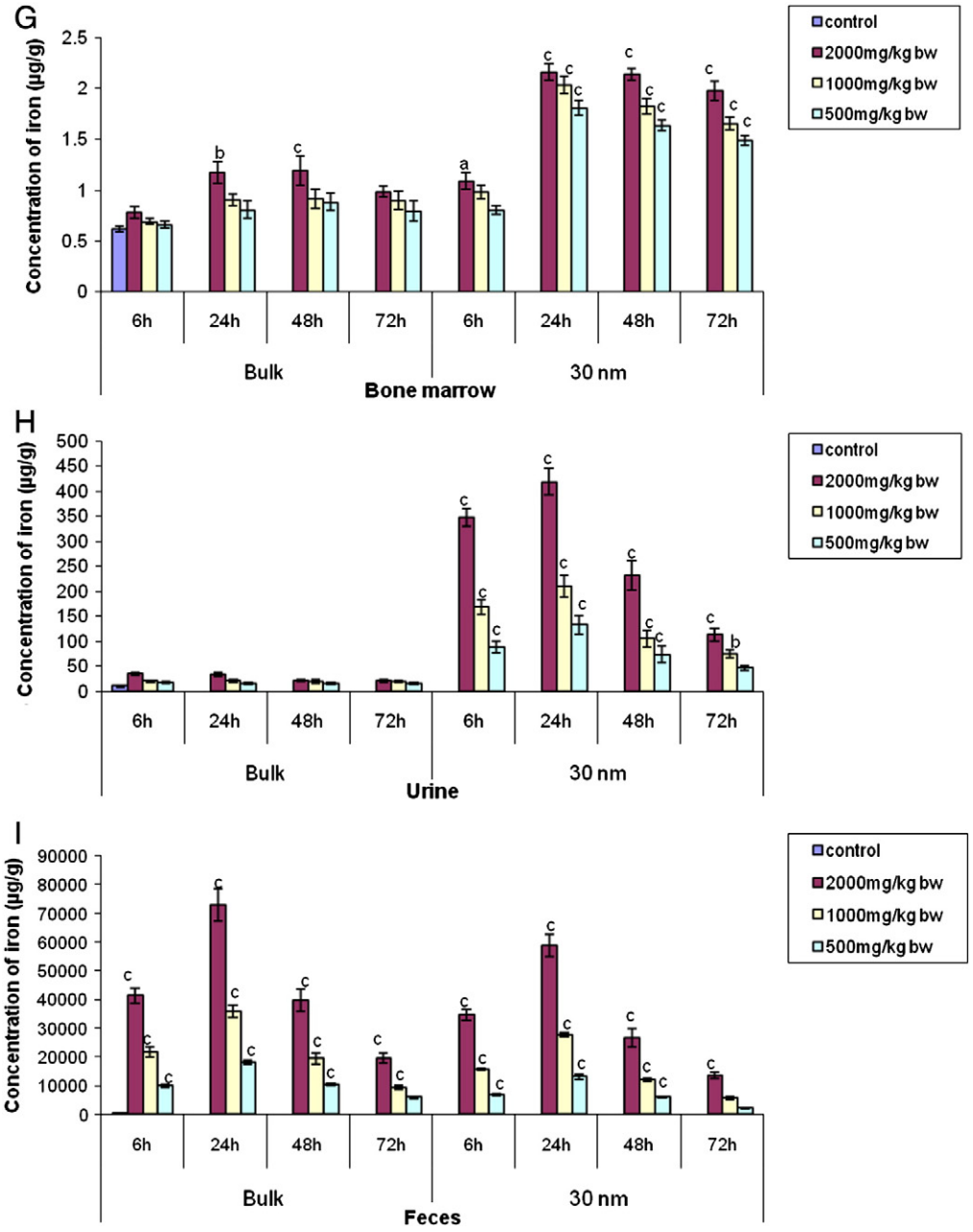

Fig. 3 (*continued*).

compounds. In the present study possibly the bioavailable Fe after exposure of Fe_2O_3-30 nm and Fe_2O_3-bulk in rats was not enough in generating ROS and thus did not cause significant genotoxicity.

In the present study it was observed that the Fe_2O_3-30 nm administered by oral route in female rats were widely distributed in various target organs, tissues, urine and feces, when measured with the atomic absorption spectrophotometry. The NMs were significantly distributed to organs such as liver, spleen, kidney, heart, blood and bone marrow. The majority of NMs was found in the liver as well as spleen and the distribution pattern was dose and time dependent, as the amount absorbed increased as the dose administered increased. Our finding suggests that Fe_2O_3-30 nm particles can easily pass across the gastrointestinal barrier and accumulates in the organs and tissues. The excretion data showed that a little quantity of NMs was excreted via urine, whereas large amount of the NMs was excreted via feces from 6–72 h. The tissue distribution of Fe with Fe_2O_3 –bulk treated rats was compared between the experimental groups and controls. Statistically significant increase was not observed in the kidney, brain, heart and blood at all the time points and doses. However significant increase was found in liver and bone marrow after 24 h; in spleen after 72 h with the 2000 mg/kg bw dose treated with Fe_2O_3-bulk. Our results indicated that only trace amount of Fe_2O_3-bulk can pass through the intestinal barrier and large amount of Fe was quickly excreted in feces at all the time points. The NMs quantity was higher in brain with the Fe_2O_3-30 nm treated groups as compared to Fe_2O_3-bulk as well as control treated groups. It is an indication that Fe_2O_3 -30 nm particles can penetrate the blood–brain barrier (BBB). This could be due to Fe binding to transferrin and the receptors are over expressed in brain endothelial cell (Descamps et al., 1996). Another reason could be that through the circumventricular organs because in the mature central nervous system, the spinal and autonomic ganglia as well as small number of other sites within the brain, called the circumventricular organs, are not protected by BBB (Kim et

al., 2006; Spencer, 2000). During the experimental period, behavioural changes were not observed in treated rats, suggesting that the slight increase in brain Fe levels may not have any toxic effects on the central nervous system. Moreover, no changes in the permeability of BBB or immunohistological changes in the brain of mice were found following intraperitoneal administration of silica coated 50 nm diameter iron oxide MNPs (Kim et al., 2006).

Other studies on the bioaccumulation of Fe after oral treatment with Fe_2O_3-30 nm have not been found in literature. However the results of intratracheally instilled $^{59}Fe_2O_3$ nanoparticles in rats at a dose of 4 mg/kg bw showed that they can easily pass through a number of tissues, distributed in many organs and accumulated in the extra pulmonary organs. The extra pulmonary Fe was significantly found in liver, spleen, heart, kidney, pancreas, testicle and brain. The highest concentration of Fe was found in liver, spleen, kidney and testicle (Zhu et al., 2008). A study demonstrated time dependent change in the bio distribution of Fe in various body tissues. When iron oxide magnetic nanoparticles were injected in male Sprague- dawley rats via tail vein, a large fraction of the injected Fe was localized in the liver and spleen and than in the brain, heart, kidney and lungs, (Jain et al., 2008). Likewise, an investigation on intragastric administration of Fe_3O_4 nanoparticles revealed time dependent distribution of Fe in various organs like heart, liver, spleen, lungs, kidneys, brain, stomach, small intestine and bone marrow in ICR mice at the single dose of 600 mg/kg bw (Wang et al., 2010a).

Fe in excess of metabolic needs is stored intracellularly as either ferritin which is found in greater quantity in the liver, spleen and bones or hemosiderin (intracellular granules). However, the liver reticuloendothelial system and intestinal mucosa are the most significant metabolic storage sites (Puntarulo, 2005). In a normal individual 30% of the total Fe is stored in the form of feritin and hemosiderin, primarily in the liver, spleen and bone marrow.

Similarly, Qian et al. (2007) found an enhancement in Fe level in rats heart which was fed with a high Fe diet. This increase could be due to the ability of heart cells to accumulate transferring and nontransferrin-bound Fe (Qian et al., 2007).

5. Conclusion

It can be concluded from our results that the orally administered Fe_2O_3–bulk particles were slightly absorbed via the gastrointestinal tract and were not significantly accumulated in the tissues after a single oral dose and rest of it rapidly cleared via feces. In contrast, Fe_2O_3-30 nm particles were easily able to pass across the intestinal barrier and the NMs mainly accumulated in the liver, spleen, kidney, heart and bone marrow. The excretion data showed that small amount of NMs was cleared via urine, whilst most of NMs were excreted via feces. The incorporation of Fe in the various tissues was in the range of 0.2-9.4% in the Fe_2O_3-30 nm treated groups and it was 0.01-2.3% in the Fe_2O_3-bulk treated groups. The accumulation depended on the doses and time intervals. The biodistribution and clearance profile of NMs showed concurrently composite events, and the dynamics of Fe concentration in different tissues, urine and feces changed with time. Hence, it can be concluded, that orally administered NMs were easily metabolized and regulated by the body's usual physiological homeostatic mechanism. The bioavailabe Fe from exposure of Fe_2O_3-30 nm and Fe_2O_3-bulk particles in rats was biocompatible and inactive in generating ROS and did not cause significant DNA damage, MN-PCEs and CAs. Fe_2O_3-30 nm NMs were well tolerated by rats after absorption through intestinal tract. This indicates that the accumulated Fe did not lead to significant genotoxicological effects. The present data adds to the information of Fe_2O_3 NMs in order to be able to interpret its toxicological implication. However more studies are warranted for careful assessment to ensure safety of Fe_2O_3 NMs in biomedical applications. Hence we need to investigate sub acute and chronic study.

Conflict of interest statement

There is no conflict of interest related to this research.

Acknowledgments

This work was financially supported by Department of Biotechnology, New Delhi, India (Grant No.BT/PR9998/NNT/28/84/2007). Further, Shailendra Pratap Singh (SRF) is grateful to Indian Council of Medical Research (ICMR), for the award of fellowship.

References

Adler, I.D., 1984. Cytogenetic tests in mammals. In: Venitt, S., Parry, J. (Eds.), Mutagenicity Testing: A Practical Approach. IRL Press, Oxford, pp. 273–306.
Auffan, M., Decome, L., Rose, J., Orsiere, T., De Meo, M., Briois, V., Chaneac, C., Olivi, L., Berge-Lefranc, J.L., Botta, A., Wiesner, M.R., Bottero, J.Y., 2006. *In vitro* interactions DMSA-coated maghemite nanoparticles and human fibroblasts: A physicochemical and cyto-genotoxical study. Environ. Sci. Technol. 40 (14), 4367–4373.
Bhattacharya, K., Davoren, M., Boertz, J., Schins, R.P., Hoffmann, E., Dopp, E., 2009. Titanium dioxide nanoparticles induce oxidative stress and DNA-adduct formation but not DNA-breakage in human lung cells. Part. Fibre Toxicol. 6, 17–22.
Bhattacharya, K., Hoffmann, E., Schins, R.F., Boertz, J., Prantl, E.M., Alink, G.M., Byrne, H.J., Kuhlbusch, T.A., Rahman, Q., Wiggers, H., Schulz, C., Dopp, E., 2012. Comparison of micro- and nanoscale Fe^{+3}-containing (Hematite) particles for their toxicological properties in human lung cells *in vitro*. Toxicol. Sci. 126, 173–182.
Brain, J.D., 1985. Macrophages in the respiratory tract (Chapter 14). In: Fishman, A.P., Fisher, A.B. (Eds.), Handbook of physiology-Sect. 3: The respiratory system. American Physiology Society, Bethesda, Maryland, pp. 447–471.
Celik, A., Ogenler, O., Comelekoglu, U., 2005. The evaluation of micronucleus frequency by acridine orange fluorescent staining in peripheral blood of rats treated with lead acetate. Mutagenesis 20, 411–415.
Collins, A.R., Oscoz, A.A., Brunborg, G., Gaivão, I., Giovannelli, L., Kruszewski, M., Smith, C.C., Stetina, R., 2008. The comet assay: topical issues. Mutagenesis 23, 143–151.
Descamps, L., Dehouck, M.P., Torpier, G., Cecchelli, R., 1996. Receptor mediated transcytosis of transferrin through blood–brain barrier endothelial cells. Am. J. Physiol. Heart Circ. Physiol. 270, H1149–H1158.
Ferrari, M., 2005. Cancer nanotechnology: opportunities and challenges. Nat. Rev. Cancer 5, 161–171.
Geiser, M., Rothen-Rutishauser, B., Kapp, N., Schurch, S., Kreyling, W., Schulz, H., Semmler, M., Im Hof, V., Hyder, J., Gehr, P., 2005. Ultrafine particles cross cellular membrane by nonphagocytic mechanism in lungs and in cultured cells. Environ. Health Perspect. 113, 1555–1560.
Gonzales-Weimuller, M., Zeisberger, M., Krishnan, M.K., 2009. Size-dependant heating rates of iron oxide nanoparticles for magnetic fluid hyperthermia. J. Magn. Magn. Mater. 321, 1947–1950.
Gua, B., Zebda, R., Drake, S.J., Sayes, C.M., 2009. Synergistic effects of co exposure to carbon black and Fe_2O_3 nanoparticles on oxidative stress in cultured lung epithelial cells. Part. Fibre Toxicol. 6, 4.
Guichard, Y., Schmit, J., Darne, C., Gaté, L., Goutet, M., Rousset, D., Rastoix, O., Wrobel, R., Witschger, O., Martin, A., Fierro, V., Binet, S., 2012. Cytotoxicity and genotoxicity of nanosized and microsized titanium dioxide and iron oxide particles in Syrian hamster embryo cells. Ann. Occup. Hyg. 56, 631–644.
Gupta, A., Gupta, M., 2005. Synthesis and surface engineering of iron oxide nanoparticles for biomedical applications. Biomaterials 26, 3995–4021.
Hafeli, U.O., Riffle, J.S., Harris-Shekhawat, L., Carmichael-Baranauskas, A., Mark, F., Dailey, J.P., 2009. Cell uptake and *in vitro* toxicity of magnetic nanoparticles suitable for drug delivery. Mol. Pharm. 6, 1417–1428.
Jain, T.K., Reddy, M.K., Morales, M.A., Leslie-Pelecky, D.L., Labhasetwar, V., 2008. Biodistribution, clearance, and biocompatibility of iron oxide magnetic nanoparticles in rats. Mol. Pharm. 5, 316–327.
Karlsson, H.L., Gustafsson, J., Cronholm, P., Möller, L., 2009. Size-dependent toxicity of metal oxide particles-a comparison between nano-and micrometer size. Toxicol. Lett. 188, 112–118.
Kim, J.S., Yoon, T.J., Yu, K.N., Kim, B.G., Park, S.J., Kim, H.W., Lee, K.H., Park, S.B., Lee, J.K., Cho, M.H., 2006. Toxicity and tissue distribution of magnetic nanoparticles in mice. Toxicol. Sci. 89, 338–347.
Kumari, M., Rajak, S., Singh, S.P., Murty, U.S.N., Mahboob, M., Grover, P., Rahman, M.F., in press. Biochemical alterations induced by acute oral doses of iron oxide nanoparticles in Wistar rats. Drug Chem. Toxicol. http://dx.doi.org/10.3109/01480545.2012.720988.
Lewinski, N., Colvin, V., Drezek, R., 2008. Cytotoxicity of nanoparticles. Small 4, 26–49.
Lobel, B., Eyal, O., Kariv, N., Katzir, A., 2000. Temperature controlled CO(2) laser welding of soft tissues: urinary bladder welding in different animal models (rats, rabbits, and cats). Lasers Surg. Med. 26, 4–12.
Lovell, D.P., Omori, T., 2008. Statistical issues in the use of the comet assay. Mutagenesis 23, 171–182.
Muhlfeld, C., Mayhew, T.M., Gher, P., Rothen-Rutishauser, B., 2007. A novel quantitative method for analyzing the distributions of nanoparticles between different tissue and intracellular compartments. J. Aerosol Med. 20, 395–407.
Murdock, R.C., Braydich-Stolle, L., Schrand, A.M., Schlager, J.J., Hussain, S.M., 2008. Characterization of nanomaterial dispersion in solution prior to *in vitro* exposure using dynamic light scattering technique. Toxicol. Sci. 101, 239–253.

Naqvi, S., Samim, M., Abdin, M.Z., Ahmed, F.J., Maitra, A.N., Prashant, C.K., Dinda, A.K., 2010. Concentration-dependent toxicity of iron oxide nanoparticles mediated by increased oxidative stress. Int. J. Nanomed. 5, 983–989.
Oberdörster, G., Maynard, A., Donaldson, K., Castranova, V., Fitzpatrick, J., Ausman, K., Carter, J., Karn, B., Kreyling, W., Lai, D., Olin, S., Monteiro-Riviere, N., Warheit, D., Yang, H., 2005. Principles for characterizing the potential human health effects from exposure to nanomaterials: elements of a screening strategy. Part. Fibre Toxicol. 2, 8.
OECD Guidelines 474 genetic toxicology (1997): micronucleus test.
OECD Guidelines 475 genetic toxicology (1997): *in vivo* mammalian bone marrow cytogenetic test-chromosome analysis.
OECD Guidelines 420 Acute oral toxicity – Fixed dose procedure (2001).
Peer, D., Karp, J.M., Hong, S., Farokhzad, O.C., Margalit, R., Langer, R., 2007. Nanocarriers as an emerging platform for cancer therapy. Nat. Nanotechnol. 2, 751–760.
Peng, S., Wang, C., Xie, J., Sun, S., 2006. Synthesis and Stabilization of Monodisperse Fe Nanoparticles. J. Am. Chem. Soc. 128, 10676–10677.
Pisanic, T.R., Blackwell, J.D., Shubayev, V.I., Finones, R.R., Jin, S., 2007. Nanotoxicity of iron oxide nanoparticle internalization in growing neurons. Biomaterials 28, 2572–2581.
Poland, C.A., Duffin, R., Kinloch, I., Maynard, A., Wallace, W.A., Seaton, A., Stone, V., Brown, S., Macnee, W., Donald, K., 2008. Carbon nanotubes introduced into the abdominal cavity of mice show asbestos-like pathogenicity in a pilot study. Nat. Nanotechnol. 3, 423–428.
Pool-Zobel, B.L., Lotzmann, N., Knoll, M., Kuchenmeister, F., Lambertz, R., Leucht, U., Schroder, H.G., Schmezer, P., 1994. Detection of genotoxic effects in human gastric and nasal mucosa cells isolated from biopsy samples. Environ. Mol. Mutagen. 24, 23–45.
Powers, K.W., Palazuelos, M., Moudgil, B.M., Roberts, S.M., 2007. Characterization of the size, shape, and state of dispersion of nanoparticles for toxicological studies. Nanotoxicology 1, 42–51.
Puntarulo, S., 2005. Iron, oxidative stress and human health. Mol. Aspects Med. 26, 299–312.
Qian, Z.M., Chang, Y.Z., Leung, G., Du, J.R., Zhu, L., Wang, Q., Niu, L., Xu, Y.J., Yang, L., Ho, K.P., Ke, Y., 2007. Expression of ferroportin1, hephaestin and ceruloplasmin in rat heart. Biochim. Biophys. Acta 1772, 527–532.
Rehn, B., Seiler, F., Rehn, S., Bruch, J., Maier, M., 2003. Investigations on the inflammatory and genotoxic lung effects of two types of titanium dioxide: untreated and surface treated. Toxicol. Appl. Pharmacol. 189, 84–95.
Sadeghiani, N., Barbosa, L.S., Silva, L.P., Azevedo, R.B., Morais, P.C., Lacavaa, Z.G.M., 2005. Genotoxicity and inflammatory investigation in mice treated with magnetite nanoparticles surface coated with polyaspartic acid. J. Magn. Magn. Mater. 289, 466–468.
Scherer, F., Anton, M., Schillinger, U., Henke, J., Bergemann, C., Krüger, A., Gänsbacher, B., Plank, C., 2002. Magnetofection: enhancing and targeting gene delivery by magnetic force *in vitro* and *in vivo*. Gene Ther. 9, 102–109.
Schmid, W., 1975. The micronucleus test. Mutat. Res. 31, 9–15.
Singh, N.P., McCoy, M.T., Tice, R.R., Schneider, E.L., 1988. A simple technique for quantitation of low levels of DNA damage in individual cells. Exp. Cell Res. 175, 184–191.
Singh, N., Manshian, B., Jenkins, G.J., Griffiths, S.M., Williams, P.M., Maffeis, T.G., Wright, C.J., Doak, S.H., 2009. NanoGenotoxicology: the DNA damaging potential of engineered nanomaterials. Biomaterials 30, 3891–3914.
Spencer, P.S., 2000. Doxorubicin and related anthracyclines. In: Spencer, P.S., Svhaumburg, H.H. (Eds.), Experimental and Clinical Neurotoxicology. Oxford University Press, New York, pp. 529–533.
Tice, R.R., Agurell, E., Anderson, D., Burlinson, B., Hartmann, A., Kobayashi, H., Miyamae, Y., Rojas, E., Ryu, J.C., Sasaki, Y.F., 2000. The single cell gel/comet assay: Guidelines for in vitro and in vivo genetic toxicology testing. Environ. Mol. Mutagen. 35, 206–221.
Verma, A., Uzuan, O., Hu, Y., Han, H.S., Watson, N., Chen, S., Irvine, D.J., Stellacci, F., 2008. Surface structure regulated cell membrane penetration by monolayer protected nanoparticles. Nat. Mater. 7, 588–595.
Wang, B., Feng, W.Y., Wang, M., Shi, J.W., Zhang, F., Ouyang, H., Zhao, Y.L., Chai, Z.F., Huang, Y.Y., Xie, Y.N., 2007. Transport of intranasally instilled Fe_2O_3 particles into the brain: Micro-distribution, chemical states, and histopathological observation. Biol. Trace Elem. Res. 118, 233–243.
Wang, Z.Y., Song, J., Zhang, D.S., 2009. Nanosized As_2O_3/Fe_2O_3 complexes combined with magnetic fluid hyperthermia selectively target liver cancer cells. World J. Gastroenterol. 15, 2995–3002.
Wang, J., Chen, Y., Chen, B., Ding, J., Xia, G., Gao, C., Cheng, J., Jin, N., Zhou, Y., Li, X., Tang, M., Wang, X.M., 2010a. Pharmacokinetic parameters and tissue distribution of magnetic Fe_3O_4 nanoparticles in mice. Int. J. Nanomedicine 21, 861–866.
Wang, L., Wang, L., Ding, W., Zhang, F., 2010b. Acute toxicity of ferric oxide and zinc oxide nanoparticles in rats. J. Nanosci. Nanotechnol. 10, 8617–8624.
Xie, J., Huang, J., Li, X., Sun, S., Chen, X., 2009. Iron oxide nanoparticle platform for biomedical applications. Curr. Med. Chem. 16, 1278–1294.
Yokel, R.A., Florence, R.L., Unrine, J.M., Tseng, M.T., Graham, U.M., Wu, P., Grulke, E.A., Sultana, R., Hardas, S.S., Butterfield, D.A., 2009. Biodistribution and oxidative stress effects of a systemically-introduced Commercial ceria engineered nanomaterial. Nanotoxicology 3, 234–248.
Zhou, Y.M., Zhong, C.Y., Kennedy, I.M., Leppert, V.J., Pinkerton, K.E., 2003. Oxidative stress and NF kappa B activation in the lungs of rats: a synergistic interaction between soot and iron particles. Toxicol. Appl. Pharmacol. 190, 157–169.
Zhu, M.T., Feng, W.Y., Wang, B., Wang, T.C., Gu, Y.Q., Wang, M., Wang, Y., Ouyang, H., Zhao, Y.L., Chai, Z.F., 2008. Comparative study of pulmonary responses to nano- and submicron-sized ferric oxide in rats. Toxicology 247, 102–111.